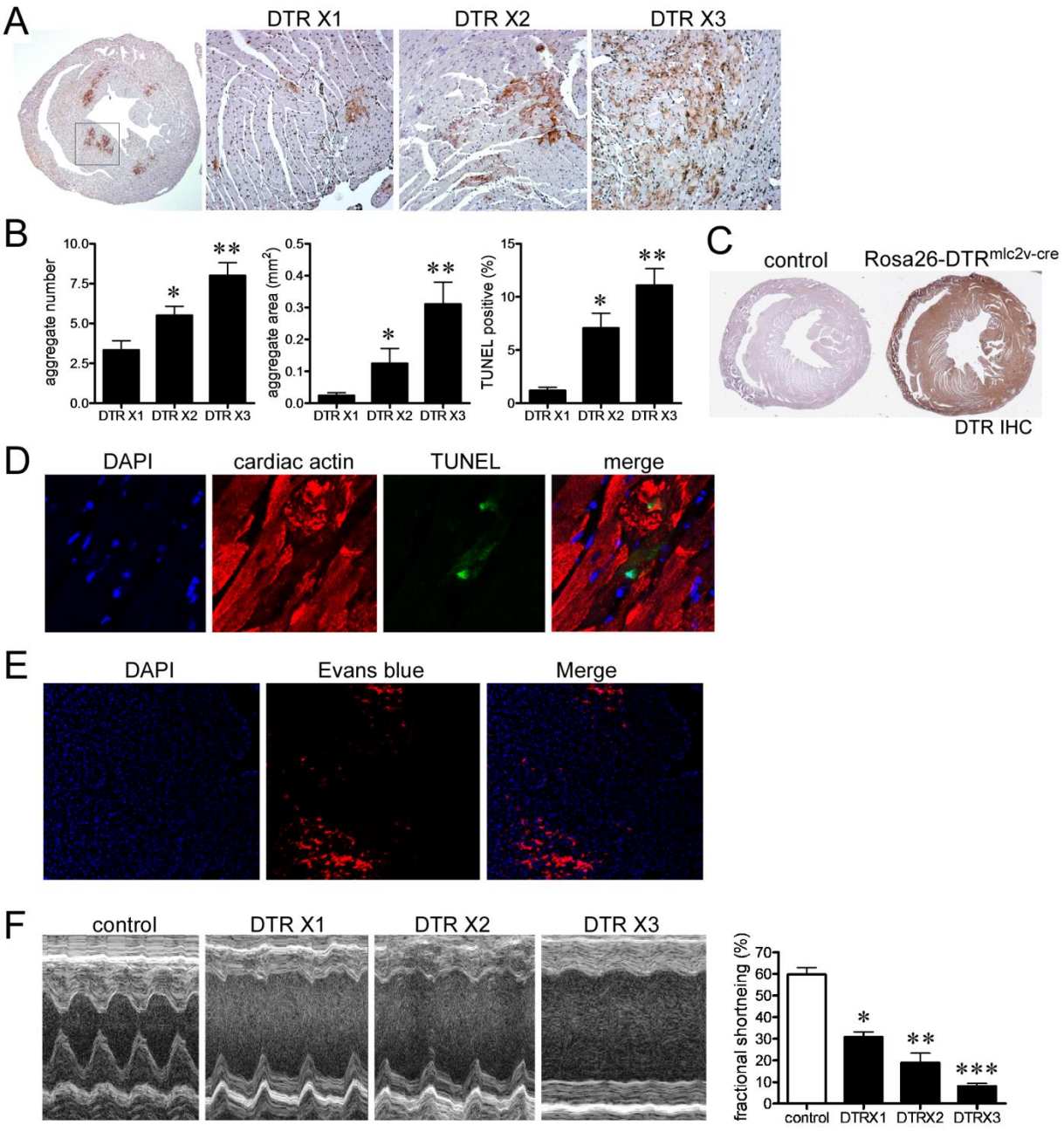

Figure S1. Cardiomyocyte cell death and ventricular dysfunction following DT induced cardiac injury. A, TUNEL staining demonstrating that the extent of cardiomyocyte cell death is proportional to the number of DT injections. **B**, Quantification of TUNEL positive aggregate number, aggregate area, and total TUNEL positive area following 1, 2, or 3 DT injections. * $p<0.05$ compared to control, **$p<0.05$ compared to all other groups. **C**, DTR IHC demonstrating uniform expression of the DTR. **D**, TUNEL and cardiac actin labeling revealing cardiomyocyte cell death immediately after DT injection. **E**, Evan's blue staining indicating the presence of necrotic cell death following DT injections. **F**, M-mode echocardiographic images of control and Rosa26-DTR$^{mlc2v\text{-}cre}$ mice immediately following 1, 2, or 3 DT injections. Quantification of fractional shortening demonstrating that the number of DT injections is proportional to the extent of ventricular dysfunction. * $p<0.05$ compared to control, **$p<0.05$ compared to control and DTRX1, ***$p<0.05$ compared to all other groups. A, low magnification and 20X objective. C, low magnification. D, 40X objective. E, 20X objective.

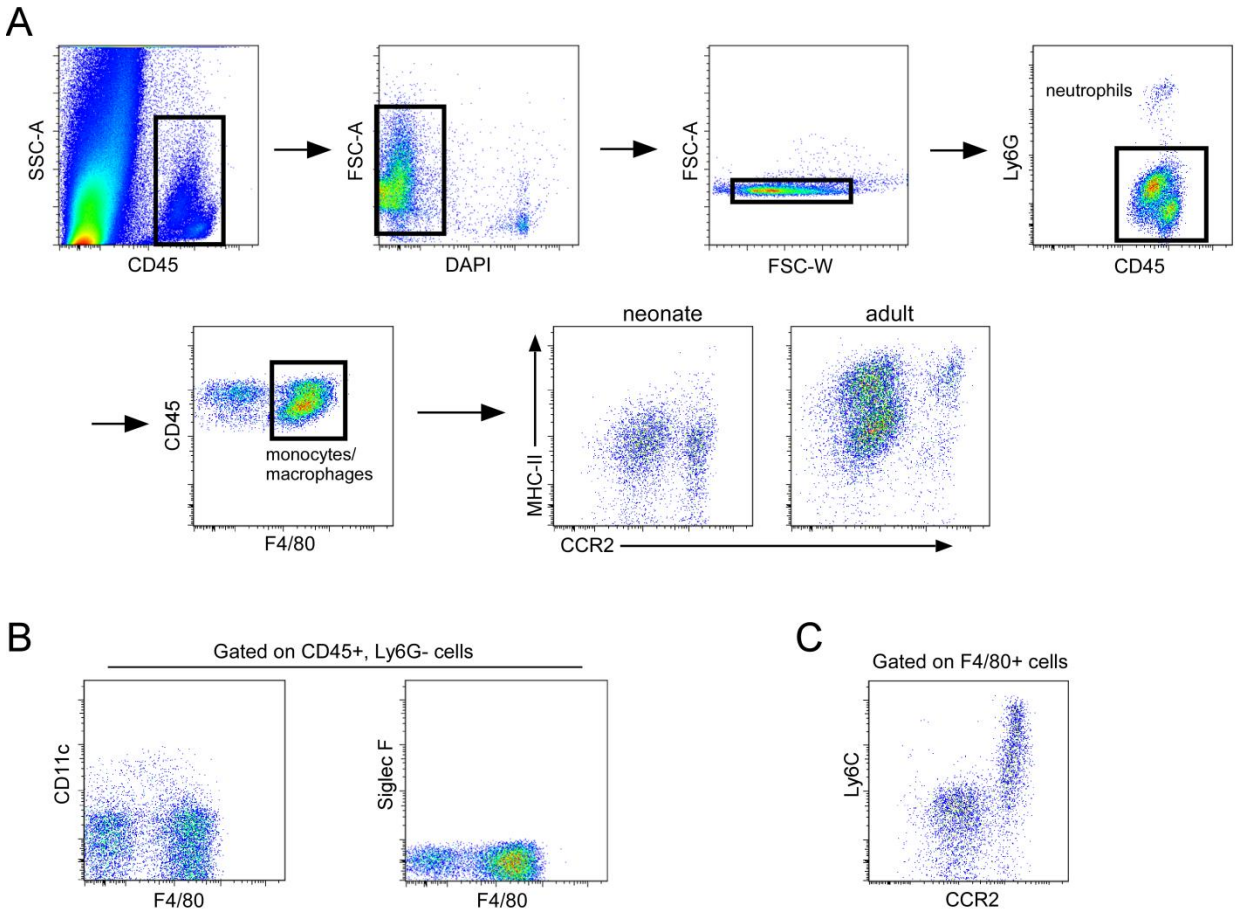

Figure S2. A, Flow cytometry gating strategy for monoycte, macrophage and neutrophil populations. **B**, CD11c and Siglec F staining revealing rare dendritic cells and absence of eosinophils in F4/80 positive population. **C**, Ly6C and CCR2 staining demonstrating that the majority of CCR2+ monocytes and macrophages co-express Ly6C.

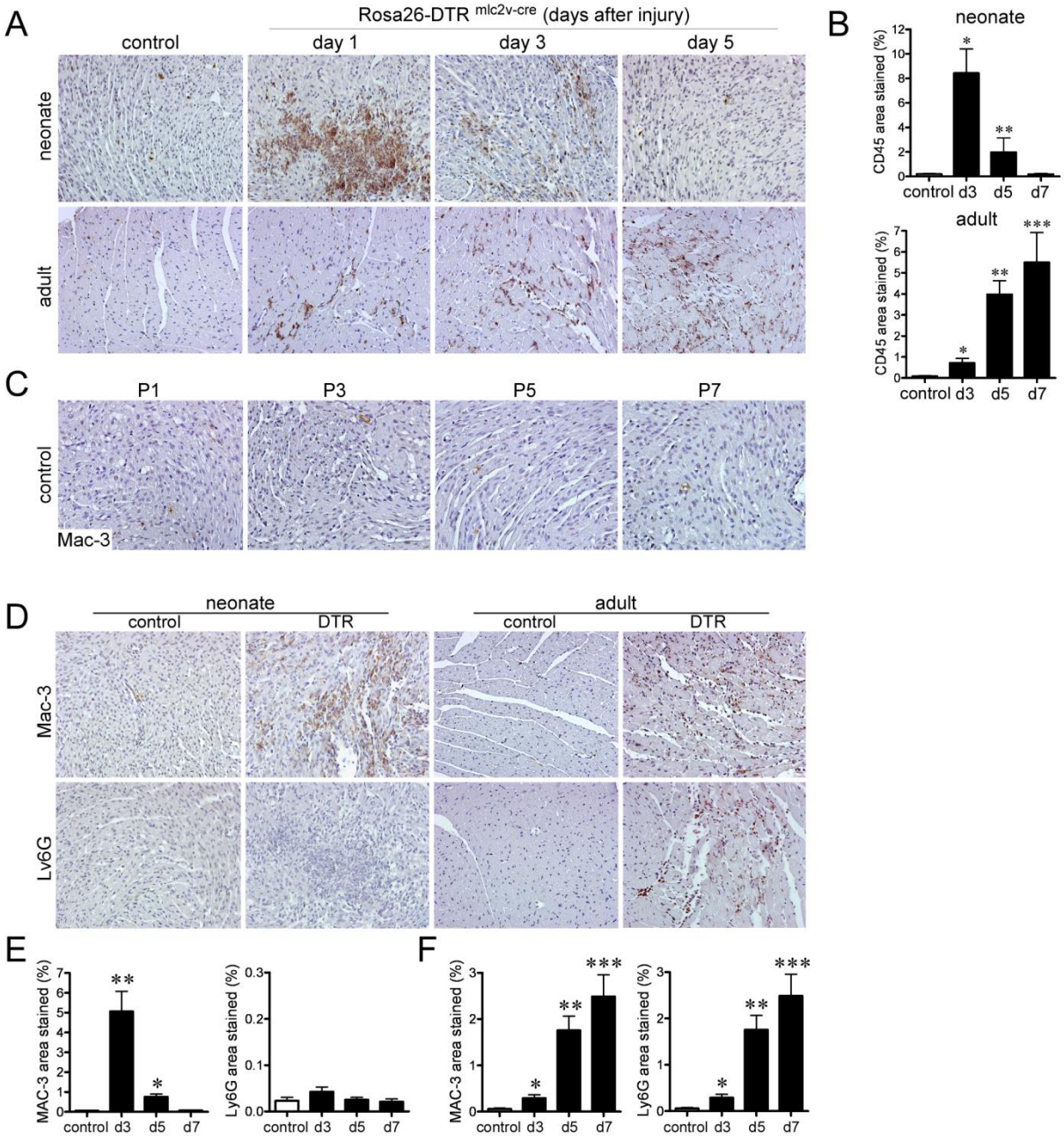

Figure S3. Distinct inflammatory responses following neonatal and adult cardiac injury. A, CD45 stained sections of control and Rosa26-DTR$^{mlc2v\text{-}cre}$ hearts following either neonatal or adult cardiac injury demonstraing distinct patterns of inflammatory cell accumulation. **B**, Quantification of CD45 immunostaining following injury in neonatal and adult hearts. **C**, Immunostaining for monocytes and macrophages (Mac-3) in control hearts demonstrating minimal change in macrophage number between P1 and P7. **D**, Immunostaining for monocytes/macrophages (Mac-3) and neutrophils (Ly6G) showing the accumulation of monocytes and macrophages following both neonatal and adult cardiac injury. In contrast, neutrophils are only found in the injured adult heart. **E-F**, Quantification of Mac-3 and Ly6G immunostaining following injury in neonatal (E) and adult (F) hearts. * $p<0.05$ compared to control, ** $p<0.05$ compared to control and day 1, *** $p<0.05$ compared to all other groups. day 1,3, and 5 denotes days following DT treatment. All mice underwent 3 DT injections. A, C, and D 20X objective.

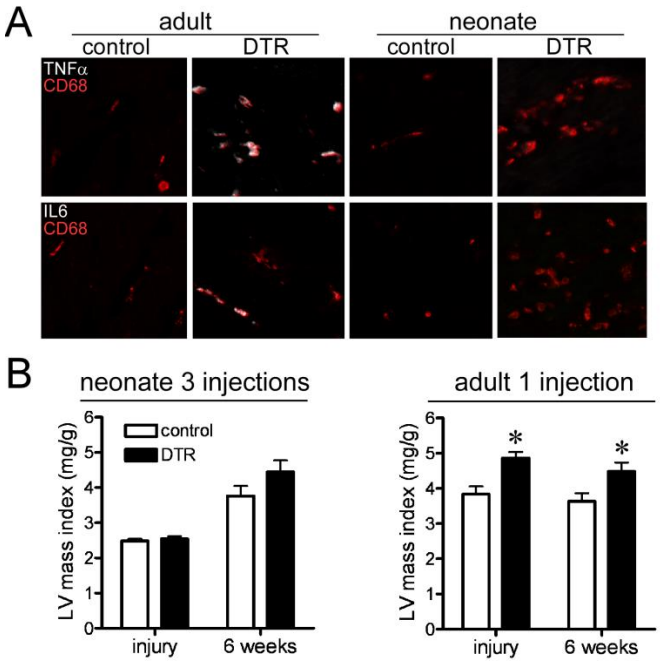

Figure S4. Pro-inflammatory chemokine expression and cardiac remodeling following neonatal and adult cardiac injury. A, Immunostaining revealing induction of TNFα and IL6 (white) in CD68 (red) positive macrophages in the injured adult heart. Macrophages within the injured neonatal heart produce minimal TNFα and IL6. **B**, Echocardiographic derived LV mass indices of neonatal (3 DT injections) and adult hearts (1 DT injection) immediately following and 6 weeks after injury

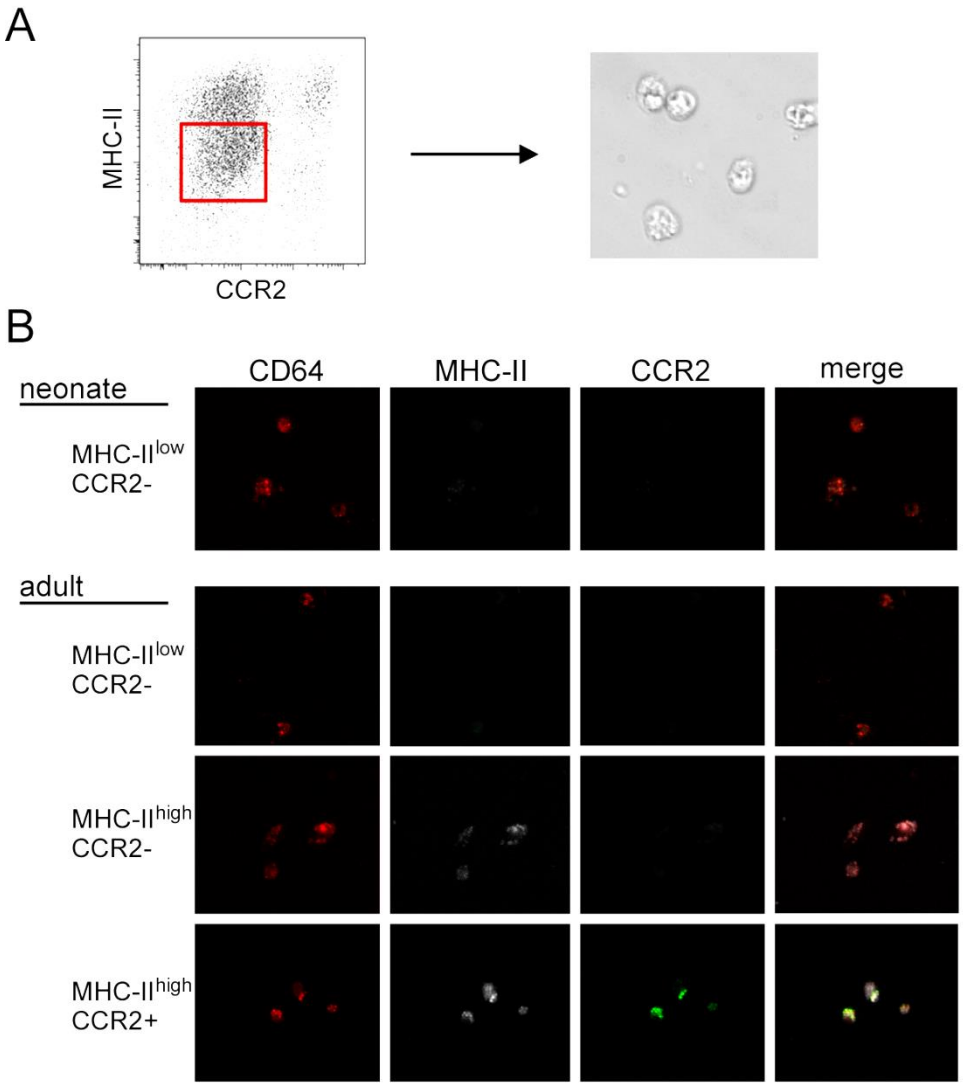

Figure S5. Characterization of cardiac macrophage populations purified by FACS. A, Examples of a flow cytometry plot and photograph of sorted cardiac macrophages. **B**, Immunostaining of sorted neonatal (top) and adult (bottom) cardiac macrophage subsets cultured for 48 hours demonstrating that cultured cardiac macrophages retain the surface expression of CD64 (red), MHC-II (white), and CCR2 (green). 40X objective.

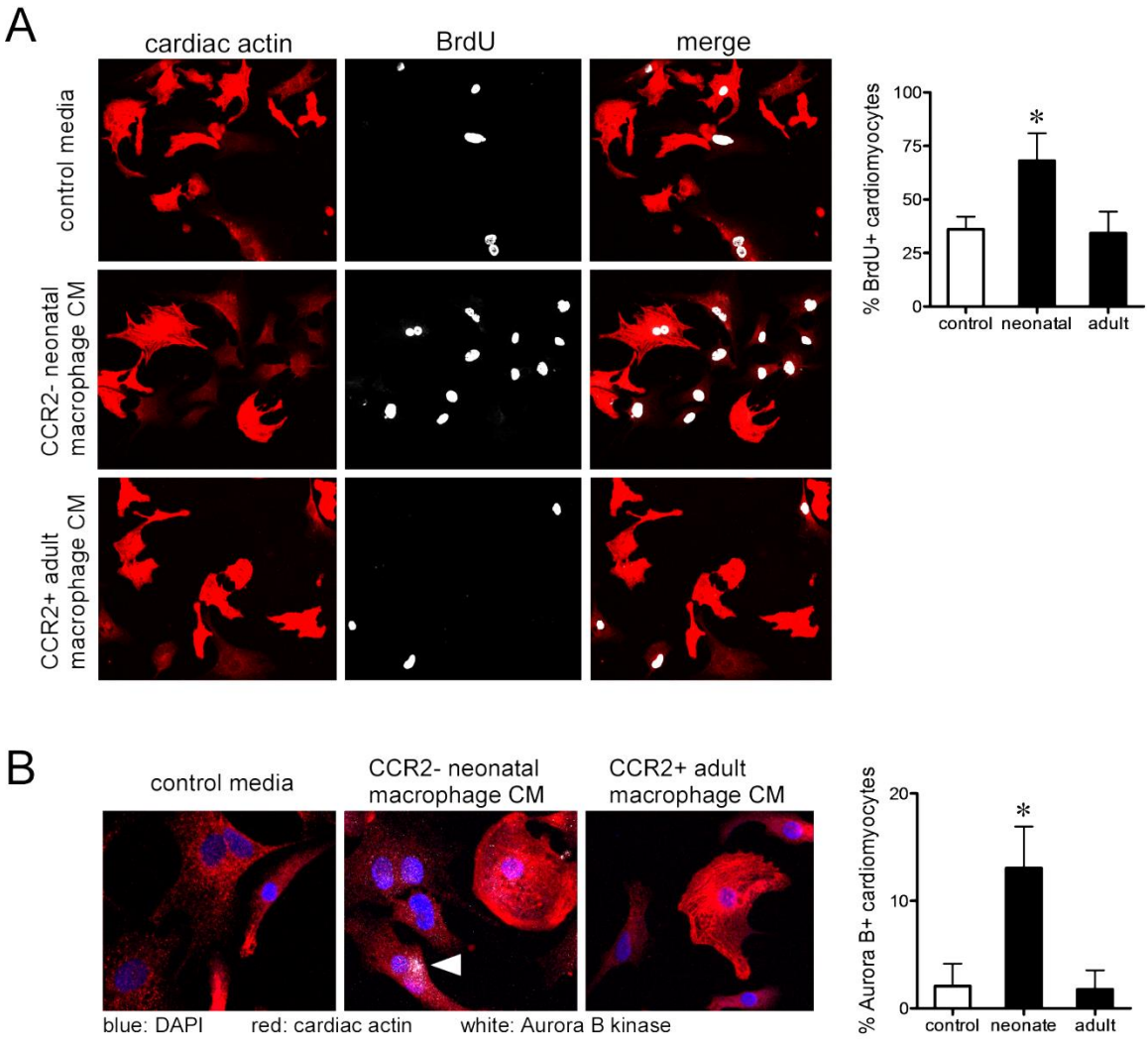

Figure S6. Neonatal cardiac macrophages stimulate NRCM proliferation. A, Immunostaining for cardiac actin (red) and BrdU (white) revealing that conditioned media (CM) collected from sorted CCR2- neonatal, but not CCR2+ adult cardiac macrophages, increases BrdU incorporation. **B**, Immunostaining for cardiac actin (red), Aurora B kinase (white, arrowhead), and DAPI staining (blue) demonstrating increased cell division in NRCMs treated with CCR2- neonatal cardiac macrophage conditioned media. A, 40X objective. B, 63X objective. . * $p<0.05$ compared to control.

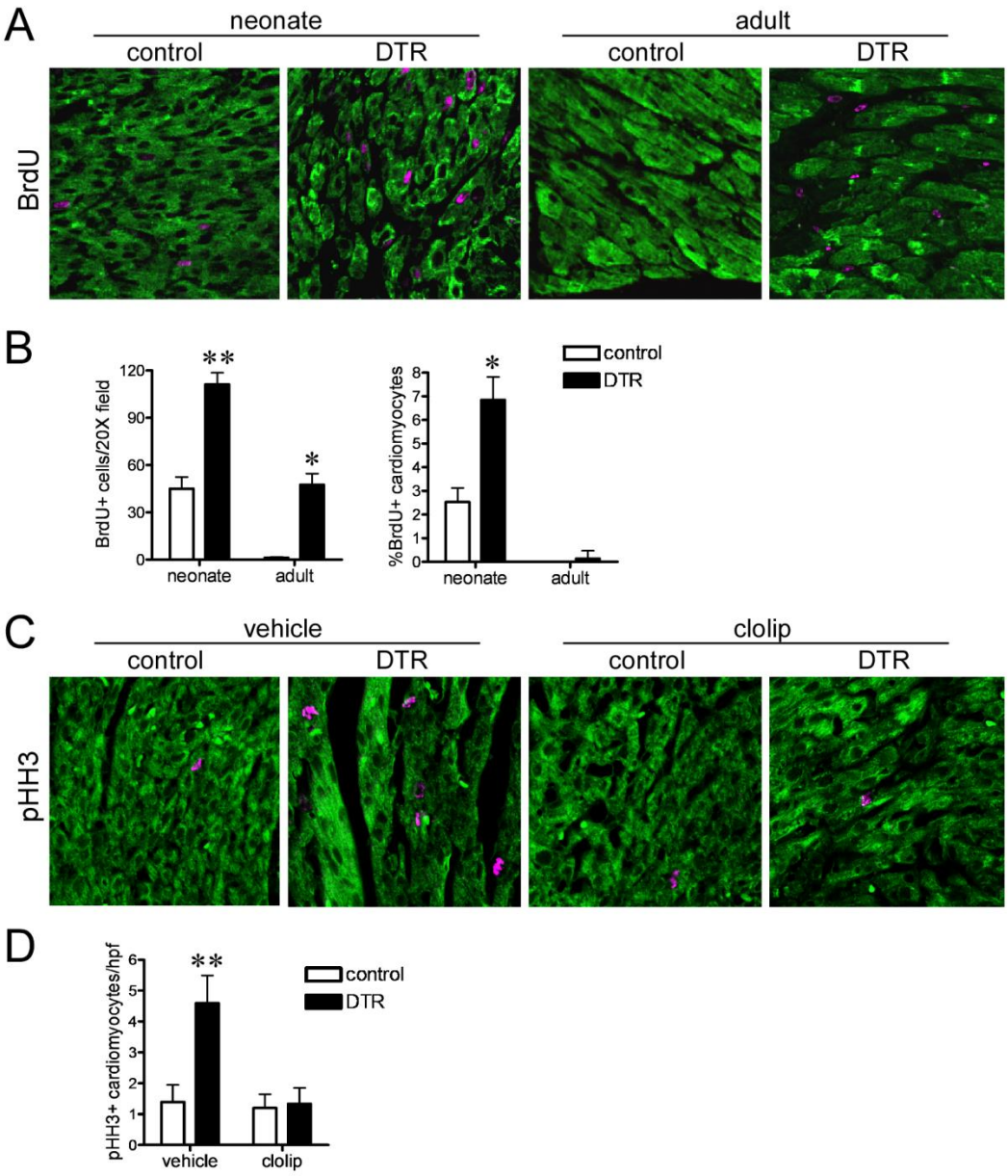

Figure S7. Increased cardiomyocyte proliferation following neonatal cardiac injury. A, BrdU (magenta) and cardiac actin (green) immunostaining showing that the neonatal heart displays a robust cardiomyocyte proliferative response following injury, while the adult heart does not display cardiomyocyte proliferation. **B**, Quantification of BrdU immunostaining revealing that while both the injured neonatal and adult heart contain increased numbers of proliferating cells, only the injured neonatal heart has increased cardiomyocyte proliferation. C, Phosphorylated histone H3 (pHH3, magenta) and cardiac actin (green) immunostaining of control and acutely injured neonatal hearts treated with either vehicle or clolip demonstrating that cardiomyocyte proliferation is dependent on macrophages. * $p<0.05$ compared to control, ** $p<0.05$ compared to all other groups.

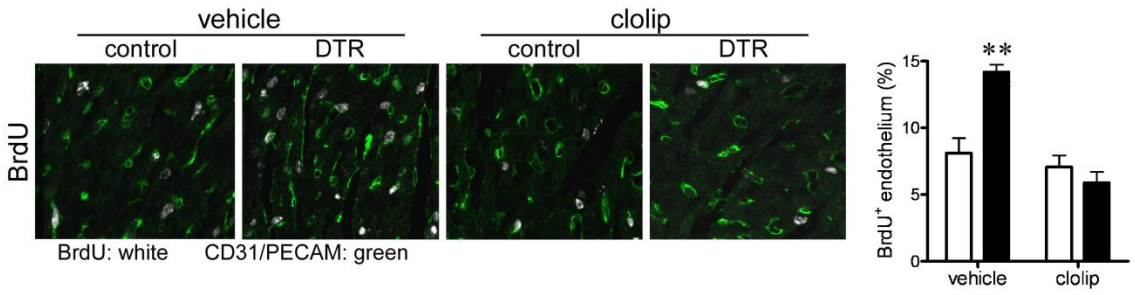

Figure S8. Macrophages are required for coronary endothelial cell proliferation in the injured neonatal heart. BrdU (white) and CD31 (green) staining revealing clolip mediated macrophage depletion blunts the proliferation of coronary endothelial cells following neonatal cardiac injury. ** $p<0.05$ compared to all other groups.

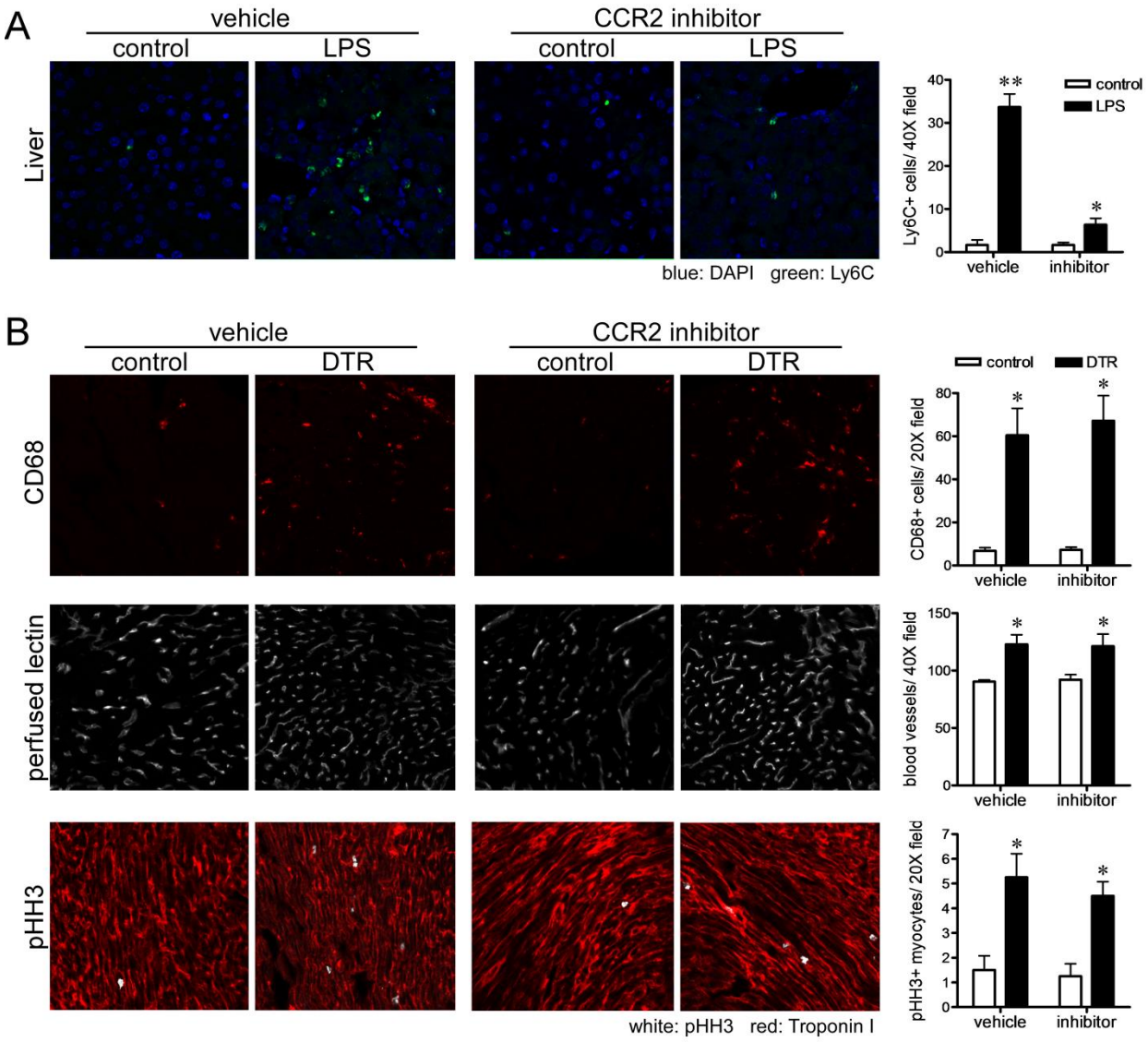

Figure S9. Monocyte recruitment is not necessary for macrophage expansion or tissue repair following neonatal cardiac injury. A, Ly6C (green) staining of livers obtain from mice treated with either vehicle or a CCR2 inhibitor demonstrating that CCR2 inhibition suppresses LPS induced monocyte recruitment. **B**, CCR2 inhibition does not affect macrophage expansion (CD68), coronary angiogenesis (perfused lectin), or cardiomyocyte proliferation (phospho-histone H3, pHH3) following neonatal cardiac injury. * $p<0.05$ compared to control, ** $p<0.05$ compared to all other groups.

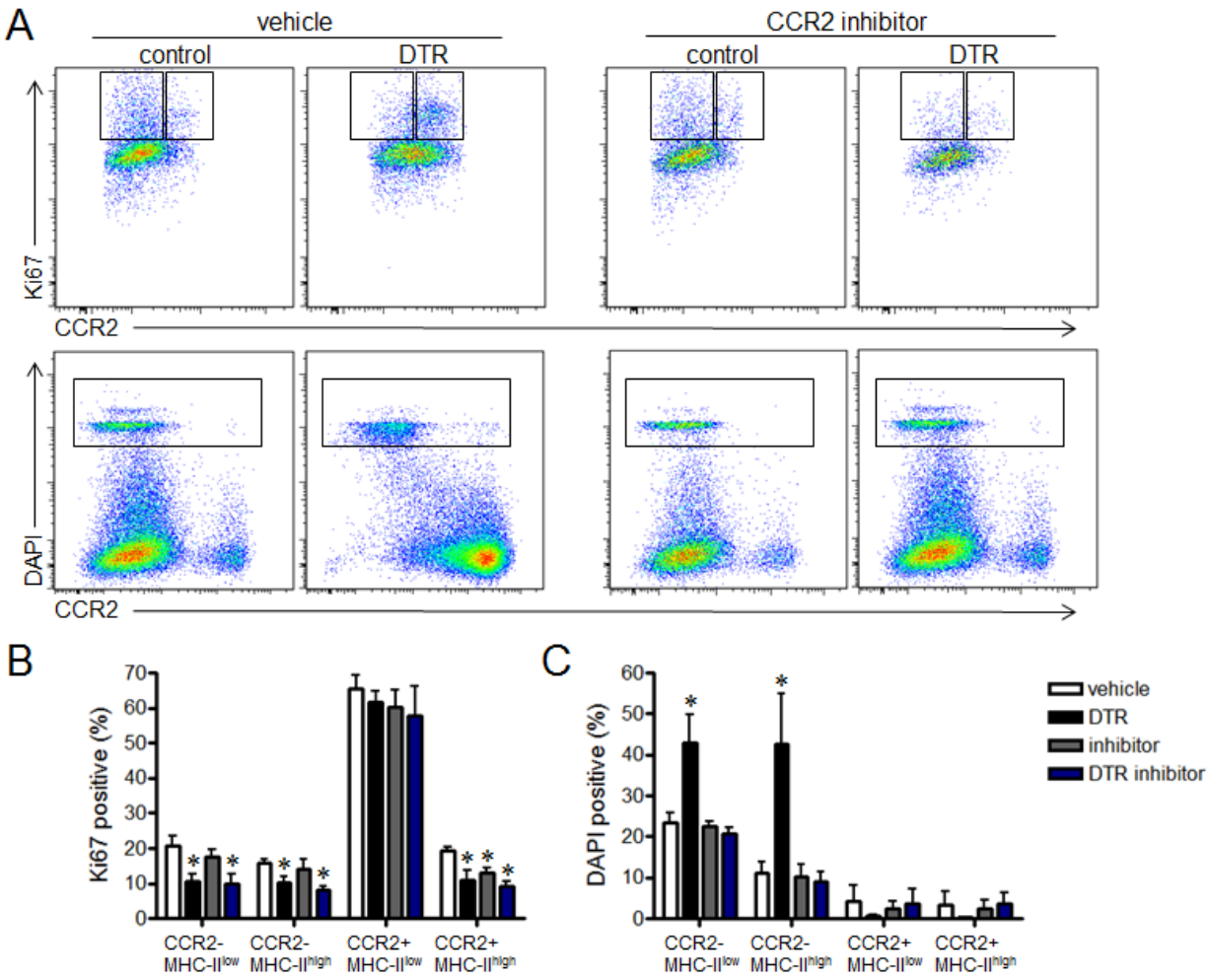

Figure S10. Recruited CCR2+ monocytes and macrophages promote cell death of resident CCR2- cardiac macrophages. A, Representative flow cytometry plots of Ki67 (top) and DAPI (bottom) staining of control and injured hearts treated with vehicle or CCR2 inhibitor. Hearts were collected immediately after 3 DT injections. Positive staining is indicated by boxes. **B,** Quantification of flow cytometry data indicating that CCR2- and CCR2+ cardiac macrophages display reduced proliferation as assayed by Ki67 staining in response to cardiac injury. CCR2- resident macrophage proliferation is not affected by the CCR2 antagonists. CCR2+ macrophage proliferation is reduced by the CCR2 antagonist. **C,** Quantification of flow cytometry data indicating that CCR2- cardiac macrophages display increased cell death following cardiac injury. CCR2 antagonist treatment prevented CCR2- resident cardiac macrophage cell death. * $p<0.05$ compared to control.

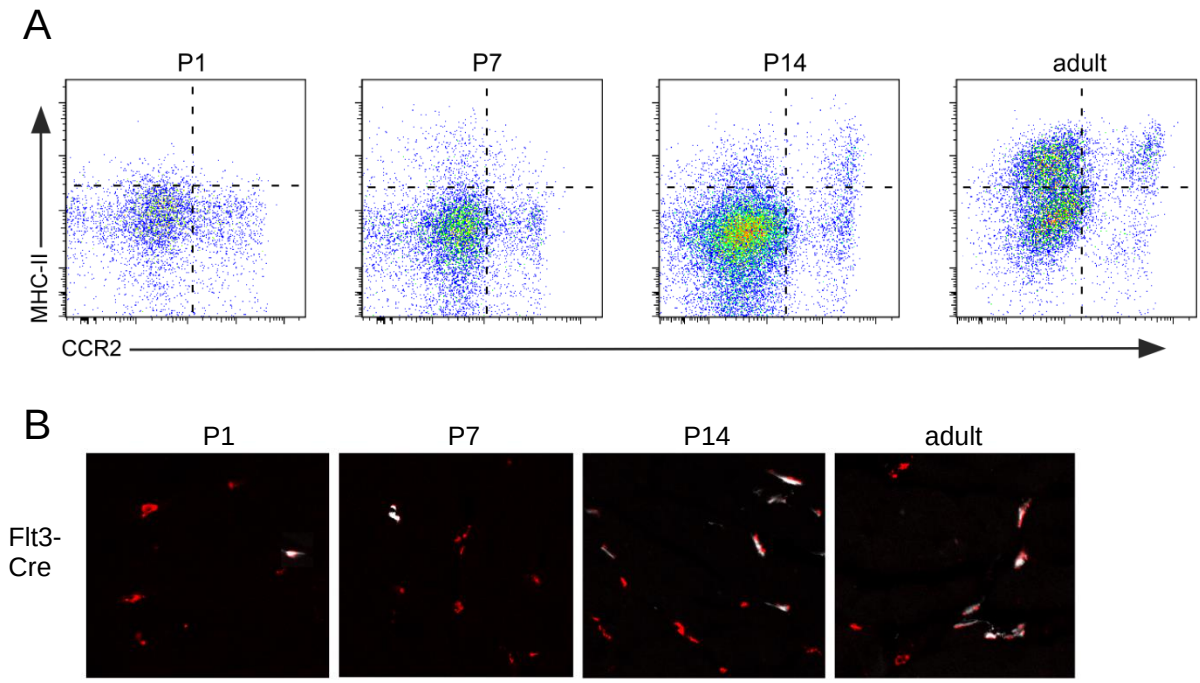

Figure S11. Resident and recruited macrophage populations in the P1, P7, P14, and adult heart. A, The P1 and P7 heart contains primarily MHC-II^{low}CCR2- macrophages and a smaller population of MHC-II^{low}CCR2+ monocytes. There is an expansion of MHC-II^{low}CCR2- macrophages and emergence of monocyte-derived MHC-II^{high}CCR2+ macrophages at P14. At 6 weeks of age (adult) the heart contains a mature complement of macrophages and monocytes**. B**, Flt3-Cre Rosa26^{td} (white) and CD68 (red) staining revealing accumulation of Flt3-Cre positive macrophages at P14 and adult stages.

SI appendix: Detailed Methods.

Mouse strains, DT cardiomyocyte ablation, CCR2 inhibition. Mice were bred and maintained at the Washington University School of Medicine and all experimental procedures were done in accordance with the animal use oversight committee. Mouse strains utilized included Mlc2v-Cre, Rosa26-DTR, Rosa26-td, Flt3-Cre, CSF1Rert-Cre, and $CCR2^{GFP}$ (1-6). All mice were genotyped according to established protocols. Macrophage lineage tracing was carried out by mating Rosa26-td mice with either Flt3-Cre or CSF1R-ertCre mice. Embryonic macrophages were labeled by treating pregnant CSF1Rert-Cre/Rosa26-td mice with 0.1mg tamoxfen per g body weight (Sigma) by oral gavage.

To ablate cardiomyocytes *in vivo*, Mlc2v-Cre mice were crossed to Rosa26-DTR mice. The resultant $Rosa26\text{-}DTR^{Mlc2v\text{-}Cre}$ animals were injected IP with 20 ng/kg of DT (Sigma). For adult mice (2-4 months) DT was diluted into 100 μl of PBS. Neonatal mice were injected with DT diluted to a final volume of 10-20 μl in PBS. 31G needles were used for all neonatal IP injections. Control animals included Rosa26-DTR/+ and Mlc2v-Cre/+. CCR2 inhibitor (Tocris RS 504393) was administered at 2 mg/kg twice daily by oral gavage.

Echocardiography. Mouse echocardiography was performed in the Washington University Mouse Cardiovascular Phenotyping Core facility using the VisualSonics 770 Echocardiography System. Avertin (0.005 ml/g) was used for sedation based on previously established methods of infarct quantification (7). 2D and M-mode images were obtained in the long and short axis views. Fractional shortening (FS), Ejection fraction (EF), LV dimension, LV mass index, and relative wall thickness were calculated using standard techniques. LV dimension was normalized to body weight. Measurements were performed on 3 independently acquired images per animal, by investigators who were blinded to experimental group. Each experimental group included at least 5 animals.

Histology, immunohistochemistry, TUNEL, Evan's blue, WGA, and CellRox staining. Tissues were fixed in 2% PFA overnight at 4°C, dehydrated in 70% ethyl alcohol, and embedded in paraffin. 4-μm sections were cut and stained with H&E. H&E, Picrosirius red and Trichrome staining was performed using standard techniques. Picrosirius red and Trichrome staining was quantified using Image J software.

For chromogenic immunohistochemical staining on paraffin sections, 4-μm sections were deparaffinized, rehydrated, peroxidase blocked, and antigen exposed by boiling in 10 mM citric acid. Primary antibodies included CD45 1:100 (BD), MAC3 1:400 (BD), and Ly6G 1:50 (BD). Biotinylated secondary antibodies were purchased from Vector Laboratories and used at 1:200. Signal was detected using the Elite ABC Kit (Vector Laboratories). CD45, MAC3, and Ly6G staining was quantified using Image J software. At least 4 sections from 4 independent samples were analyzed in blinded fashion. For all other immunostaining assays tissues were fixed in 2% PFA overnight at 4°C, embedded in OCT, infiltrated with sucrose, frozen, and 10- to 12-μm cryosections were cut. Primary antibodies used were: Aurora B kinase (1:200) Abcam, BrdU 1:100 (DAKO), cardiac actin 1:400 (Sigma), human HB-EGF/DTR 1:200 (RD), PECAM 1:200 (BD), pHH3 (1:100, Sigma), CD68 1:400 (Serotec), CCR2 1:100 (Abgent), MHC-II 1:200 (biolegend), IL1β 1:200 (BD), IL6 1:200 (RD), MCP1 1:200 (biolegend), TNFα 1:200 (biolegend), Troponin I 1:100 (Abcam). Immunofluorescence was visualized on a Zeiss confocal microscopy system. BrdU positive cells, blood vessel density, and macrophages were quantified by examining at least 4 similarly oriented sections from 4 independent samples in blinded fashion.

TUNEL staining was performed on paraffin-embedded sections immediately following DT injections (Roche). To quantify TUNEL staining sections, sections were photographed at low magnification using the high resolution Pathscan imaging system. The total TUNEL positive area, aggregate size and number were quantified using Image J software. Serum Troponin I concentration was measured by ELISA (Life Sciences). To identify necrotic cells Evan's blue

was injected IP 48 hrs prior to sacrifice and cryosections were imaged using a Zeiss confocal Microscope. To quantify cardiomyocyte cross-sectional area paraffin sections were stained with rhodamine conjugated WGA (Vector labs), visualized on a Zeiss confocal microscope, and measurements preformed using Zeiss Axiovision software. CellRox (Invitrogen) staining was performed on fresh frozen sections per manufacturer instructions, visualized, and quantified using Zeiss confocal microscope and software. For all experiments, at least 4 sections from 4 independent samples were analyzed in blinded fashion.

Cardiomyocyte isolation and contractility studies. Ventricular cardiomyocytes from control or Rosa26-DTR$^{Mlc2v\text{-}Cre}$ mice injured as neonates or adults were isolated as previously described. Cardiomyocytes were isolated 6 weeks following DT treatment. Following isolation, the cardoimyocyte suspension was washed 3 times in Wittenberg Isolation medium containing 116 mM NaCl, 5.4 mM KCl, 8 mM $MgCl_2$, 1 mM NaH_2PO_4, 1.5 mM KH_2PO_4, 4 mM $NaHCO_3$, 12 mM glucose, 21 mM HEPES, and 2 mM glutamine, supplemented with 1X essential vitamins (GIBCO), 1X essential amino acids (GIBCO), 50mg/ml BSA, 12.5mg/ml Taurine, and with increasing concentrations of CaCl2 (150μM, 400μM, and 900μM). The cells were then washed with Tyrode's solution containing 137 mM NaCl, 5.4 mM KCl, 0.16 mM NaH_2PO_4, 10 mM glucose, 1 mM CaCl2, 0.5 mM $MgCl_2$, 5 mM HEPES, and 3 mM $NaHCO_3$, pH 7.3–7.4. Freshly isolated cardiomyocytes were transferred to a recording chamber mounted on the stage of a Nikon inverted microscope and superfused at 60ml/hour with normal Tyrode's solution. The cells were allowed to settle for 5 minutes and were subsequently paced (5-10V) at 0.5 Hz for 5 minutes before recording. All experiments were performed at room temperature. Video images of individual cardiomyocyte contractions were acquired using a Myocam camera (IonOptix), and a Fourier transform was applied to the dark/light contrast of the A and I bands to calculate the sarcomere length. Length traces were subsequently analyzed with the Ion Wizard software (IonOptix). To assess contractile reserve cardiomyocytes were treated with 10 μM isoproterenol

(Sigma). Each experimental group included 4 mice and at least 20 cardiomyocytes were examined per mouse.

Clodronate mediated macrophage depletion, flow cytometry, and macrophage culture. Vehicle control (lipsomomes only) and liposomal clodronate was produced as previously described (18 mg/ml)(9). To deplete macrophages in the neonatal heart vehicle control or 15 μl clodronate was injected IP on postnatal day 1 and 5. DT was injected IP on postnatal days 2-4.

For flow cytometry experiments, mice were euthanized by cervical disolocation. Hearts were then perfused with cold PBS, finely minced, and digested with Collagenase D (Roche) and DNAse I for 15-20 min at 37C. The digested material was filtered through 40 mM filters and pelleted by centrifugation (400xg for 5 min at 4C) in HBSS supplemented with 2% FCS + 0.2% BSA. Red blood cells were lysed in ACK lysis buffer (Invitrogen) and then resuspended in FACS buffer (PBS containing 2% FCS and 2 mM EDTA). Blood was collected into heparinized syringes, RBCs lysed, and the remaining cells resuspended in FACS buffer. Samples were incubated with Fc block (BD), labeled with fluorescently conjugated antibodies (supplemental table 1) for 30 min at 4C, and washed twice in FACS buffer. Flow cytometry analysis was done on either a LSRII analyzer. After gating on CD45+ cells, doublets were excluded, and live cells were analyzed using DAPI dead/live exclusion. Gating strategies are summarized in Figure S1.

Cell sorting was performed using a MoFlo sorting instrument (Beckman Coulter). For RNA isolation, macrophages were directly sorted into the QLT buffer and RNA isolated using the RNeay micro kit (Qiagen) per manufacturer's instructions. For culture experiments, samples were sorted directly into DMEM 10% FBS. Macrophages were plated at a density of 20,000 cells/well of a 96 well plate and allowed to adhere for 24 hours. To obtain macrophage conditioned media, cell were incubated in DMEM 1% FBS for 48 hours. To measure TNFα production macrophages were stimulated with vehicle control (PBS) or 20ng/ml LPS for 24 hrs

and the media assayed using an TNFα ELISA (R&D). IL1β release was measured by stimulating cells with PBS or 10ng/ml LPS for 24 hrs followed by treatment with ATP for 30 mins and the media assayed using an IL1β ELISA (R&D).

To determine whether macrophage conditioned media was capable of promoting neonatal cardiomyocyte proliferation, neonatal rat ventricular cardiomyocytes were isolated as previously described(10). Cells were allowed to adhere for 24 hrs, washed 3 times with DMEM 1% FBS, and incubated with either control media or macrophage conditioned media for 48 hrs. BrdU was added 24 hrs prior to harvest. BrdU incorporation was measured using an ELISA assay (Roche) per manufacturer's instructions. To determine whether macrophage conditioned media promoted angiogenesis, MCECs(11) were serum starved, stimulated with control media or macrophage conditioned media for 24 hrs, and plated on Matrigel (BD) at a density of $2X10^4$ cells/ml in a 24 well plate format. Photographs were acquired 8 hrs after plating and the number of tube segments/10X field quantified. For the ELISA, proliferation, and angiogenesis experiments, 4 independent samples were included in each experimental group and assays were repeated at least 2 times to ensure technical accuracy.

RNA isolation, cDNA synthesis and, quantitative RT-PCR. RNA was isolated from 4 independent biological samples using the RNeasy kit (QIAGEN). cDNA was synthesized using the high capacity cDNA reverse transcription kit (Ambion). Quantitative RT-PCR was performed on an ABI 7200 machine using either TaqMan based or SYBR green based assays. Taqman probes for *Anp, Bnp,* and *Hprt* were purchased from Applied Biosystems. SYBR green primers were obtained from IDT. All samples were normalized to *Hprt* or *Gapdh* and then scaled relative to controls, where control samples were set at a value of 1. Thus, results for all experimental samples were graphed as relative expression compared with control.

Statistical analysis. Data are expressed as mean ± SD. Student's *t* test or ANOVA was used for comparisons between groups. Log rank test was used for Kaplan-Meier analyses. *P*-

values of less than 0.05 were considered significant. Bonferroni correction was performed when multiple hypotheses were tested. In these cases, the type I error (alpha=0.05) was split equally amongst each test.

Supplemental Table 1. Antibodies used for flow cytometry.

Antibody	Clone	Supplier
CD45	30-F11	Biolegend
CD64	X54-5/7.1	Biolegend
F4/80	C1:A3-1 and BM8	Biolegend
MHC-II (I-Ab)	AF6-120.1	Biolegend
CCR2	475301	R&D
MerTK	108928	R&D
Ly6G	1A8	Biolegend
Ly6C	HK1.4	Biolegend
CD11c	N418	Biolegend
Siglec F	E50-2440	BD Biosciences
CD115	AFS98	Biolegend
CD16/CD32	2.4G2	BD Biosciences
Ki67	SolA15	eBiosciences

Reference List

1. Boyer SW, Schroeder AV, Smith-Berdan S, Forsberg EC (2011) All hematopoietic cells develop from hematopoietic stem cells through Flk2/Flt3-positive progenitor cells. Cell Stem Cell 9: 64-73.

2. Epelman S et al (2014) Embryonic and Adult-Derived Resident Cardiac Macrophages Are Maintained through Distinct Mechanisms at Steady State and during Inflammation. Immunity 40: 91-104.

3. Buch T et al (2005) A Cre-inducible diphtheria toxin receptor mediates cell lineage ablation after toxin administration. Nat Methods 2: 419-426.

4. Madisen L et al (2010) A robust and high-throughput Cre reporting and characterization system for the whole mouse brain. Nat Neurosci 13: 133-140.

5. Qian BZ et al (2011) CCL2 recruits inflammatory monocytes to facilitate breast-tumour metastasis. Nature 475: 222-225.

6. Chen J et al (1998) Selective requirement of myosin light chain 2v in embryonic heart function. J Biol Chem 273: 1252-1256.

7. Kanno S et al (2002) Echocardiographic evaluation of ventricular remodeling in a mouse model of myocardial infarction. J Am Soc Echocardiogr 15: 601-609.

8. Lavine KJ, Kovacs A, Weinheimer C, Mann DL (2013) Repetitive myocardial ischemia promotes coronary growth in the adult mammalian heart. J Am Heart Assoc 2: e000343.

9. Seiler P et al (1997) Crucial role of marginal zone macrophages and marginal zone metallophils in the clearance of lymphocytic choriomeningitis virus infection. Eur J Immunol 27: 2626-2633.

10. Ma X et al (2012) Impaired autophagosome clearance contributes to cardiomyocyte death in ischemia/reperfusion injury. Circulation 125: 3170-3181.

11. Barbieri SS, Weksler BB (2007) Tobacco smoke cooperates with interleukin-1beta to alter beta-catenin trafficking in vascular endothelium resulting in increased permeability and induction of cyclooxygenase-2 expression in vitro and in vivo. FASEB J 21: 1831-1843.